Electronic Supplementary Material (ESI) for Reaction Chemistry & Engineering.

Electronic Supplementary Information for "Estimating Speciation of Aqueous Ammonia Solutions of Ammonium Bicarbonate: Application of Least Squares Methods to Infrared Spectra"

Federico Milella[a], Marco Mazzotti[a,*]

[a]*Institute of Process Engineering, ETH Zurich, 8092 Zurich, Switzerland*

Abstract

This is the *Electronic Supplementary Information* to the article "Estimating Speciation of Aqueous Ammonia Solutions of Ammonium Bicarbonate: Application of Least Squares Methods to Infrared Spectra". This document provides:

1. ATR-FTIR calibration sets of aqueous ammonia solutions of ammonium bicarbonate;
2. Optimal parameter sets of the ATR-FTIR calibration methods based on maximum peak height or on peak area;
3. ^{13}C NMR spectroscopic analyses of aqueous solutions of NH_4Cl(aq) and $KHCO_3$(aq) and of NH_4HCO_3(aq);
4. Evidence of CO_2(aq) formation in an aqueous solution of NH_4HCO_3(aq);
5. Solid-Liquid Flash Calculations in the $CO_2-NH_3-H_2O$ system;
6. Illustration of the Experimental Setup.

ATR-FTIR Calibration Sets of Aqueous Ammonia Solutions of Ammonium Bicarbonate

The set of standard concentrations of aqueous ammonia solutions of ammonium bicarbonate used for the ATR-FTIR calibration procedure [1] are reported in Table. 1.

Fig. 1 shows the range of ammonium bicarbonate concentrations explored that covers the supersaturated as well as the undersaturated region of the phase diagram. The solid lines in Fig. 1

---

[*] I am corresponding author

Email addresses: `milellaf@ipe.mavt.ethz.ch` (Federico Milella), `marco.mazzotti@ipe.mavt.ethz.ch` (Marco Mazzotti)

Compound	**Concentration** [mol/kg$_\mathrm{w}$]				**Temperature** [°C]			
Sample No.	1	2	3	4	1	2	3	4
$\mathrm{NH_4HCO_3}$ (aq) ($m^\circ_{\mathrm{NH_3}} = 0$ m)	1.76	2.02	2.31	2.64	5- 25	$10^\dagger$ - 25	$10^\dagger$ - 25	$16^\dagger$ - 25
$\mathrm{NH_4HCO_3}$ (aq) ($m^\circ_{\mathrm{NH_3}} = 1.2$ m)	2.64	2.89	3.05	3.17	5 - 25	$8^\dagger$ - 25	$12^\dagger$ - 25	$14^\dagger$ - 25
$\mathrm{NH_4HCO_3}$ (aq) ($m^\circ_{\mathrm{NH_3}} = 1.8$ m)	3.06	3.27	3.42	3.53	5 - 25	$6^\dagger$ - 25	$8^\dagger$ - 25	$13^\dagger$ - 25

Table 1: Set of standard concentrations of aqueous ammonia solutions of ammonium bicarbonate used for the ATR-FTIR calibration (see Fig. 1); the variable $m^\circ_{\mathrm{NH_3}}$ refers to the nominal ammonia concentration in the solvent in mol/kg$_w$. The symbol (†) refers to the temperature value corresponding to the onset of primary nucleation.

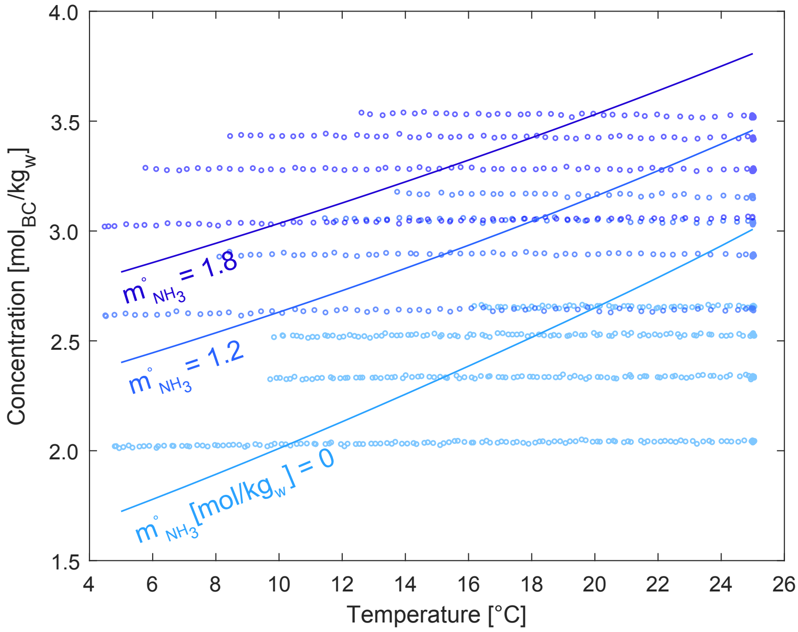

Figure 1: Set of ATR-FTIR calibrations of aqueous ammonia solutions of ammonium bicarbonate in the temperature range 5-25 °C; the variable $m^\circ_{\mathrm{NH_3}}$ refers to the nominal ammonia concentration in the solvent in mol/kg$_w$. The IR spectra of the mixtures at constant solute concentration have been collected for calibration purposes (see Table. 1). The concentration data after nucleation has been omitted and excluded from the calibration sets.

represent the solubility of ammonium bicarbonate at different nominal ammonia concentration in the solvent, $m^\circ_{\mathrm{NH_3}}$.

Optimal Parameter Sets of the ATR-FTIR Calibration Methods Based on Maximum Peak Height or on Peak Area

The sets of optimal model parameters for the ATR-FTIR calibration methods based on maximum peak height and on maximum peak area are reported in Table 2.

^{13}C NMR Spectroscopic Analyses of Aqueous Solutions of $NH_4Cl(aq)$ and $KHCO_3(aq)$ and of $NH_4HCO_3(aq)$

^{13}C NMR Spectroscopic analyses on have been used to qualitatively assess the extent of speciation of aqueous solutions of $NH_4Cl(aq)$ and $KHCO_3(aq)$ and of $NH_4HCO_3(aq)$ used for the validation of the Classical Least Squares (CLS) methodology proposed in this work.

Moving from top to bottom, Fig. 2 shows the ^{13}C NMR spectra of an equimolar aqueous solution of $NH_4Cl-KHCO_3$ (2.0 m), an aqueous solution of ammonium bicarbonate (2.0 m), and an aqueous solution of ammonium carbamate (1.6 m) at 25 °C respectively. The ^{13}C NMR peaks located at 168.24 ppm (indicated with a red dashed line in Fig. 2), 165.62 ppm, and 160.36 ppm refer to the carbonate ion, the carbamate ion, and the bicarbonate ion respectively. Because the equilibration between the carbonate and bicarbonate ions is rapid, the peaks for these two ions appear as a single peak whose position depends on the relative amounts of the two ions [2].

For the case of the first two solutions, i.e. the solution of $NH_4Cl(aq)$ and $KHCO_3(aq)$, and the solution of $NH_4HCO_3(aq)$, no significant speciation of the HCO_3^- ion can be acknowledged, therefore these mixtures have been used to validate the CLS methodology. On the contrary, for the case of the solution of ammonium carbamate, the significant extent of speciation of the carbon atoms into carbamate and carbonate ions prevented the use of this mixture for validation.

Evidence of $CO_2(aq)$ Formation in an Aqueous Solution of $NH_4HCO_3(aq)$

Due to the equilibrium reaction of eqn (1) taking place in an aqueous solution of ammonium bicarbonate, $CO_2(aq)$ is formed in solution (see Fig. 3).

$$CO_2(aq) + H_2O \rightleftharpoons H^+ + HCO_3^- \tag{1}$$

Additionally, the evaporation of $CO_2(g)$ leads to a significant pressure increase in the reactor (up to 6 barg depending on the temperature and $CO_2(aq)$ concentration).

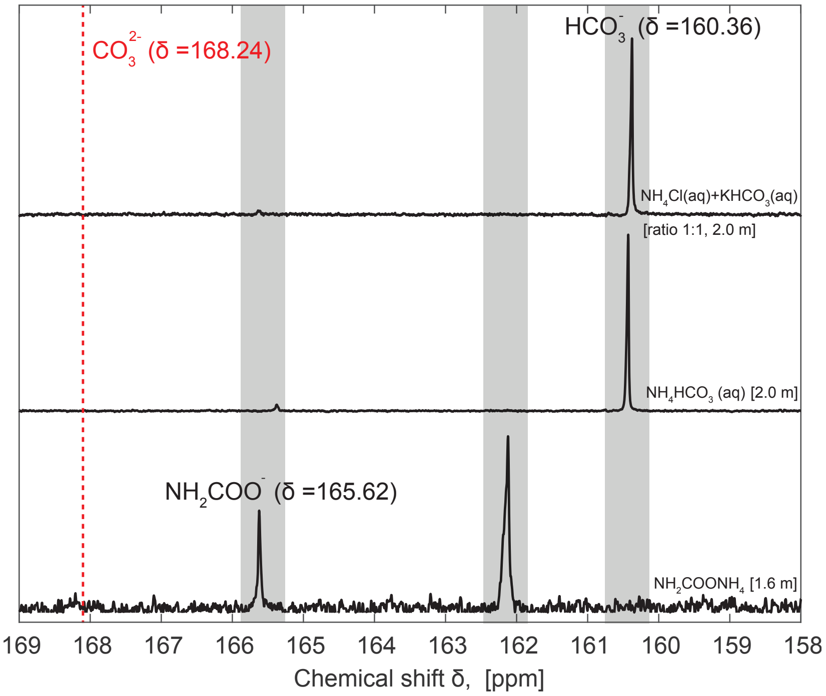

Figure 2: From top to bottom: ^{13}C NMR spectrum of an equimolar aqueous solution of $NH_4Cl-KHCO_3$ (2.0 m), an aqueous solution of ammonium bicarbonate (2.0 m), and an aqueous solution of ammonium carbamate (1.6 m) at 25 °C respectively. The carbonate, bicarbonate and carbamate ions' peaks are located at 168.24 ppm, at 165.62 ppm, and at 160.36 ppm respectively. For the case of the ammonium carbamate solution, the fast equilibration of the bicarbonate and carbonate ions leads to a single peak whose position depends on the relative amounts of the bicarbonate and carbonate ions [2].

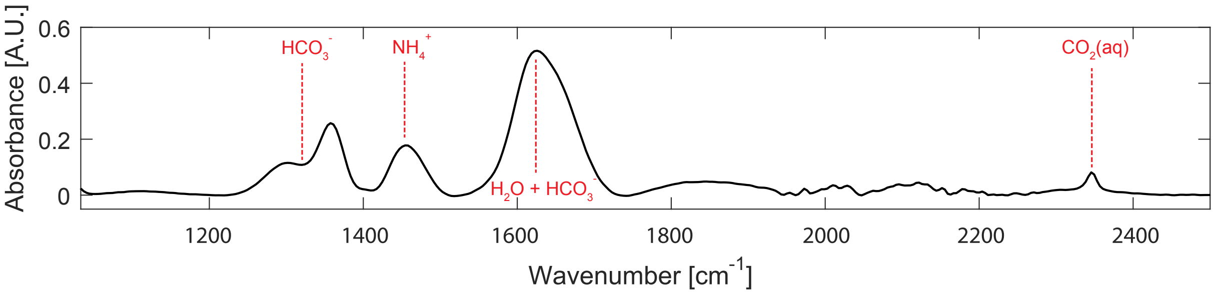

Figure 3: IR spectrum of an aqueous solution of ammonium bicarbonate at 25 °C. The analysis of the spectrum reveals the presence of the NH_4^+ (located at 1445 cm^{-1}) and HCO_3^- (located at 1355 cm^{-1}) ions and the solvent (water, located at 1640 cm^{-1}). Additionally, the presence of CO_2(aq) can be inferred by the visible asymmetric C=O stretching band of CO_2 located at 2343 cm^{-1} in the infrared spectrum of the mixture.

Solid-Liquid Flash Calculations in the $CO_2-NH_3-H_2O$ system

A main problem in the calculation of solid-liquid equilibrium is that the number and types of solid phases at equilibrium are not known in advance. This problem is solved by using a stepwise procedure, where the Gibbs function minimization (and stability analysis of the obtained solution) is used compute the number of stable phases in the system. Furthermore, it is assumed that, under the operating conditions investigated, no vapor-liquid or vapor-liquid-solid equilibria is established. This leads to the following algorithm, where **S** is the vector of supersaturations of the salts in the $CO_2-NH_3-H_2O$ system:

Algorithm 1 Computation of the Solid-Liquid Equilibria

```
Require: Temperature and total composition of the system (equivalent $CO_2$, $NH_3$, and $H_2O$
  weight fractions).
  The thermodynamic supersaturations S of all possible solid phases in the system are then calculated.
  if S is less or equal to 1 (for all salts) then
    return equilibrium liquid speciation of the system
  else
    while S is greater than 1 do
      identify the salt with the maximum degree of supersaturation
      based on the knowledge of the most unstable salt, compute the equilibrium liquid speciation
      and the solid fraction of the compound allowed to precipitate ($S = 1$).
    end while
    return equilibrium liquid speciation of the system and the solid fraction(s) of the relevant
    salt(s) precipitated (invariant points, i.e. two solid phases in equilibrium with a liquid phase,
    have also been detected).
  end if
```

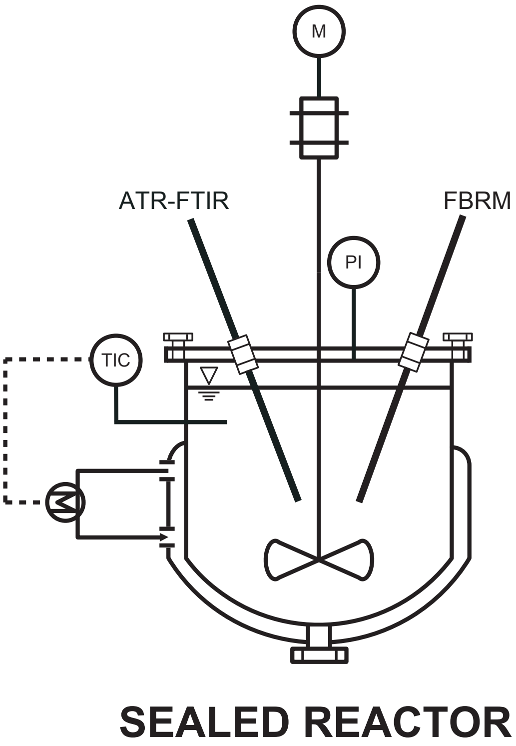

Figure 4: Illustration of the experimental setup.

Illustration of the Experimental Setup

Fig. 4 shows the experimental setup that consists of a sealed vessel equipped with a magnetically driven stirrer and with on-line monitoring tools such as the ATR-FTIR and the FBRM. The probes are connected to the reactor by means of custom-made pressure connectors installed in the lid of the vessel.

Species	**Method**	**Wavenumber**	$\hat{p}_0$	$\hat{p}_1$	$\hat{p}_2$	$\mathbf{R}^2$
		[cm^{-1}]	[mol/kg$_\mathrm{w}$]	[mol/(kg$_\mathrm{w}$A.U.)]	[mol/(kg$_\mathrm{w}$°C)]	[-]
$\mathbf{NH_4}^+$	Peak Area	$1324 \leq \tilde{\nu} \leq 1522$	$(-2.506 \pm 0.216) \cdot 10^{-1}$	$(1.344 \pm 0.011) \cdot 10^{-1}$	$(1.122 \pm 0.053) \cdot 10^{-2}$	0.9985
	Maximum Peak Height	$\tilde{\nu} = 1458$	$(-5.068 \pm 0.099) \cdot 10^{-1}$	10.27 ± 0.03	$(3.638 \pm 0.220) \cdot 10^{-3}$	0.9918
$\mathbf{HCO_3}^-$	Peak Area	$1156 \leq \tilde{\nu} \leq 1466$	$(4.818 \pm 1.718) \cdot 10^{-2}$	$(4.856 \pm 0.035) \cdot 10^{-2}$	$(2.945 \pm 0.480) \cdot 10^{-3}$	0.9990
	Maximum Peak Height	$\tilde{\nu} = 1365$	$(-9.160 \pm 0.092) \cdot 10^{-1}$	7.426 ± 0.020	$(3.245 \pm 1.900) \cdot 10^{-4}$	0.9937
$\mathbf{CO_3}^{\mathbf{2}-}$	Peak Area	$1208 \leq \tilde{\nu} \leq 1492$	$(-5.989 \pm 0.337) \cdot 10^{-2}$	$(1.798 \pm 0.012) \cdot 10^{-2}$	$(2.331 \pm 0.110) \cdot 10^{-3}$	0.9974
	Maximum Peak Height	$\tilde{\nu} = 1395$	$(-6.850 \pm 0.229) \cdot 10^{-2}$	1.827 ± 0.008	$(1.685 \pm 0.070) \cdot 10^{-3}$	0.9943
$\mathbf{NH_3}$	Peak Area	$1033 \leq \tilde{\nu} \leq 1178$	$(7.230 \pm 0.059) \cdot 10^{-1}$	$(4.119 \pm 0.020) \cdot 10^{-1}$	$(3.278 \pm 0.350) \cdot 10^{-3}$	0.9988
	Maximum Peak Height	$\tilde{\nu} = 1111$	$(3.119 \pm 0.049) \cdot 10^{-1}$	25.70 ± 0.09	$(3.977 \pm 0.250) \cdot 10^{-3}$	0.9976

Table 2: Sets of optimal vector parameters $\hat{\mathbf{p}}$ for the ATR-FTIR calibration models based on maximum peak height or on maximum peak area. Coefficients are provided with 95 % confidence bounds.

References

[1] J. Cornel, C. Lindenberg, M. Mazzotti, Quantitative Application of in Situ ATR-FTIR and Raman Spectroscopy in Crystallization Processes, Ind. Eng. Chem. Res. 47 (14) (2008) 4870–4882. doi:10.1021/ie800236v.

[2] P. E. Holmes, M. Naaz, B. E. Poling, Ion Concentrations in the $CO_2-NH_3-H_2O$ System from ^{13}C NMR Spectroscopy, Ind. Eng. Chem. Res. 37 (8) (1998) 3281–3287. doi:10.1021/ie9707782.